# Analysis of TerraSAR-X data sensitivity to bare soil moisture, roughness, composition and soil crust

M. Aubert, N. Baghdadi, Mehrez Zribi, A. Douaoui, C. Loumagne, Frédéric Baup, Mohammad El Hajj, Sébastien Garrigues

Author-produced version of the article published in Remote Sensing Of Environment, 2011, 115(8), 1801-1810.
The original publication is available at http://www.sciencedirect.com/
doi : 10.1016/j.rse.2011.02.021

# Characterization of the soil surface by TerraSAR-X imagery

**M. Aubert[(1)], N. Baghdadi[(1)], M. Zribi[(2)], A. Douaoui[(3)], C. Loumagne[(4)], F. Baup[(2)], M. El Hajj[(5)], S. Garrigues[(6)]**

*[(1)]CEMAGREF – UMR TETIS, 34196 Montpellier (France), Email: nicolas.baghdadi@teledetection.fr; maelle.aubert@teledetection.fr, tel : + 33 4 67 54 87 07*

*[(2)]CESBIO, 31401 Toulouse (France), Email : Mehrez.Zribi@latmos.ipsl.fr; frederic.baup@cesbio.cnes.fr*

*[(3)]Laboratoire Eau, roche et plante, Centre univeristaire de Khémis miliana, 44225 (Algérie), Email : abdouaoui@yahoo.fr*

*[(4)]CEMAGREF – UR HBAN, 92163 Antony (France), Email : cecile.loumagne@cemagref.fr*

*[(5)]NOVELTIS, 31520 Ramonville-Saint Agne (France), Email : mahmoud.elhajj@noveltis.fr*

*[(6)]CNES, 31000 Toulouse (France), Email: sebastien.garrigues@cnes.fr*

**Corresponding author:**

Maëlle Aubert

500 rue Jean-François Breton, 34093 Montpellier Cedex 5, France

Tel : +33 4.67.54.87.54

Fax: +33 4.67.54.87.00 (France)

Email : maelle.aubert@teledetection.fr

Author-produced version of the article published in Remote Sensing Of Environment, 2011, 115(8), 1801-1810.
The original publication is available at http://www.sciencedirect.com/
doi : 10.1016/j.rse.2011.02.021

**ABSTRACT**

Soils play a key role in shaping the environment and in risk assessment. We characterized the soils of bare agricultural plots using TerraSAR-X (9.5 GHz) data acquired in 2009 and 2010. We analyzed the behavior of the TerraSAR-X signal for two configurations, HH-25° and HH-50°, with regard to several soil conditions: moisture content, surface roughness, soil composition and soil-surface structure (slaking crust).

The TerraSAR-X signal was more sensitive to soil moisture at a low (25°) incidence angle than at a high incidence angle (50°). For high soil moisture (>25%), the TerraSAR-X signal was more sensitive to soil roughness at a high incidence angle (50°) than at a low incidence angle (25°).

The high spatial resolution of the TerraSAR-X data (1 m) enabled the soil composition and slaking crust to be analyzed at the within-plot scale based on the radar signal. The two loamy-soil categories that composed our training plots did not differ sufficiently in their percentages of sand and clay to be discriminated by the X-band radar signal.

However, the TerraSAR-X signal has the potential to detect low variations of soil moisture at the within-plot scale. Consequently, the spatial distribution of slaking crust could be detected when soil moisture variation is observed between soil crusted and soil without crust. Indeed, areas covered by slaking crust could have greater soil moisture and consequently a greater backscattering signal than soils without crust.

***Keywords:*** *soil moisture, roughness, soil composition, slaking crust, X-band, TerraSAR-X images, within field plot scale.*

Author-produced version of the article published in Remote Sensing Of Environment, 2011, 115(8), 1801-1810.
The original publication is available at http://www.sciencedirect.com/
doi : 10.1016/j.rse.2011.02.021

## 1. INTRODUCTION

Floods, drought and erosion are major issues for risk assessment. In the context of sustainable development, soil management is important for environmental and socioeconomic applications. Hence, there is a need for continuous information about key soil parameters to predict and understand these natural hazards [Wu & Wang, 2007]. Slaking crust (the disintegration of ploughed clods) is a key factor that controls runoff and erosion because of its influence on infiltration capacity [Cazenave & Valentin, 1992; Govers et al., 2000; King & Le Bissonnais, 1992; Le Bissonnais & Singer, 1992]. Similarly, by conditioning the distribution of rainfall between infiltration, surface retention and runoff [Auzet et al., 2005; Cerdan et al., 2002; Valentin, 2005], soil moisture and surface roughness play an important role in risk assessment [Loumagne et al., 1991, 2001; Oudin et al., 2003]. Nevertheless, monitoring and modeling these soil surface characteristics remain difficult because of their substantial variation over space and time [Boiffin et al., 1988; Brown et al., 1990; Zobeck & Onstad, 1987].

In this context, satellite imagery is a powerful tool that can provide accurate and repetitive spatial data. Synthetic-aperture radar (SAR) techniques are particularly useful because they make it possible to monitor soil parameters under any weather conditions [Dobson & Ulaby, 1986; Fung, 1994; Hallikainen et al., 1985; Ulaby et al., 1986]. For bare agricultural soils, the backscattered radar signal depends strongly on the geometric characteristics (roughness) and dielectric properties (moisture content, soil composition) of the soil. Many studies using data collected by space and airborne SAR scatterometers and model simulations have already shown the potential of radar data to retrieve soil parameters (roughness and moisture) [Baghdadi et al., 2002, 2006, 2007, 2008b; Dobson & Ulaby, 1986; Fung et al., 1992; Holah et al., 2005; Le Hegarat et al., 2002; Oh, 2004; Shi et al., 1997; Srivastava et al., 2003-2009; Ulaby et al., 1978; Zribi et al., 2005; Zribi & Dechambre, 2002].

Author-produced version of the article published in Remote Sensing Of Environment, 2011, 115(8), 1801-1810.
The original publication is available at http://www.sciencedirect.com/
doi : 10.1016/j.rse.2011.02.021

Whatever the SAR configuration, the radar signal follows a logarithmic function with the soil-surface roughness [Fung, 1994; Ulaby et al., 1986]. Ulaby et al. (1978) have shown that the influence of surface roughness decreases with increasing radar frequency. The dynamics of the relationship between the radar signal and roughness parameter are stronger in the L-band than in the C- and X-bands [Baghdadi et al., 2008a; Ulaby et al., 1986] Moreover, SAR data are more sensitive to soil roughness at high incidence angles [Baghdadi et *al.,* 2008a, 2008b; Zribi & Dechambre, 2002].

The SAR signal increases with increasing soil moisture for values between 0 and 35-40% [Baghdadi et al., 2007; Holah et al., 2005]. Beyond this threshold, the backscattering coefficient becomes constant and then decreases with increasing soil moisture [Holah et al., 2005]. Several studies in the C-band, with the SAR configuration fixed at a single polarization, have shown that the sensitivity of the radar signal to soil moisture is greater at low and medium incidence angles than at high incidence angles (approximately 0.2 dB/% for HH-20°-37° and approximately 0.1 dB/% for HH-39°) [Baghdadi et al., 2006, 2008b; Beaudoin et al., 1990; Srivastava et al., 2003; Zribi & Dechambre, 2002].

However, few studies have been conducted in the X-band. The first results based on microwave measurements in the X-band have shown that an incidence angle of 25° is appropriate to observe soil moisture [Singh, 2005]. For the TerraSAR-X sensor, Paris Anguela et al. (2010) have found that the sensitivity of the radar signal to soil moisture is approximately 0.35 dB/% for the HH-25° configuration.

The surface area of soil particles in a soil depends on the particle sizes which control the percentage of free and bound water [Srivastava et al., 2009]. Few studies have analyzed the response of the radar signal to soil composition in terms of grain-size distribution (percentages of sand and clay), but several studies have evaluated the effect of salt content on the radar signal. These studies have underlined the influence of salt concentrations on dielectric properties [Aly et

Author-produced version of the article published in Remote Sensing Of Environment, 2011, 115(8), 1801-1810.
The original publication is available at http://www.sciencedirect.com/
doi : 10.1016/j.rse.2011.02.021

al., 2007; Lasne et al., 2008; Shao et al., 2003; Taylor, 1996]. Several studies have recommended high radar wavelengths (L-band) and wet soil conditions for better discrimination between saline and non-saline soil. Under the wettest conditions (soil moisture greater than 30%), the effects of salinity on the C-band are important for sandy soil but do not appear clearly in soils of finer composition due to salt retention by fine particles, such as silt and clay [Aly et al., 2007]. Also, grain-size distribution has an effect on dielectric behavior over the entire frequency range (1.4 to 18 GHz) and is most pronounced at frequencies below 5 GHz [Hallikainen et al., 1985]. In the C-band, decreasing soil clay content increases the sensitivity of the radar signal to soil moisture (0.22 dB/% for clay soil: 49% clay, 35% silt and 16% sand; 0.33 dB/% for loamy soil: 17% clay, 48% silt and 35% sand) [Ulaby et al., 1978]. Because the distribution of grain sizes controls the amount of free water that interact with the incident microwave, the amount of free water gives significant contribution to SAR backscatter [Srivastava et al., 2006, 2009]. Recent methodology developed to retrieve soil moisture is based on this amount of free water which is controled by the grain size distribution [Srivastava et al., 2009].

In the X-band at HH polarization, Prakash et al. (2009) have shown a relationship between the specular scattering coefficient for bistatic scatterometer data and the sand percentage in the soil when surface roughness is less than 1.4 cm. For the TerraSAR-X sensor, Paris Anguela et al. (2010) have also shown (based on one plot and one SAR acquisition at HH-25°) that the SAR signal is 3 dB weaker for a soil composition with more clay (32% clay, 64.5% silt and 3.5% sand) than for a soil with less clay (17% clay, 79% silt and 4% sand).

Because soil slaking depends primarily on material properties (moisture, organic-matter content and carbonate content) and decreases infiltration rates, the backscattered radar signal may be sensitive to this soil parameter. Nevertheless, few studies have examined the effect of soil slaking on the radar signal. In the X-band, Stolp & Janse (1986) have carried out a multiple linear regression to relate the backscattering coefficient (HH-15°) to the degree of slaking, the direction

Author-produced version of the article published in Remote Sensing Of Environment, 2011, 115(8), 1801-1810.
The original publication is available at http://www.sciencedirect.com/
doi : 10.1016/j.rse.2011.02.021

of tillage and the incidence angle. Their results are promising and provide good estimates of the degree of slaking (with an accuracy between 78% and 56%).

Finally, soil parameters are usually estimated from SAR imagery at plot or watershed scales. Few studies have been conducted at the within-plot scale. In fact, the speckle effects and low resolution (between 10 and 30 m) of the first-generation SAR data (ERS, RADARSAT-1 and ASAR) prevented the analysis of small-scale variations. The high spatial resolution of the TerraSAR-X sensor (1 m) provides access to soil-surface heterogeneities at a finer scale. Baghdadi et al. (2008a) have already mentioned signal variations from TerraSAR-X images within agricultural plots. Quantitative analysis were not conducted, but only observations were given from photo-interpretation of SAR images. Paris Anguela et al. (2010) have made a preliminary diagnostic with an analysis from only one bare agricultural plot and in using only one TerraSAR image. In the present work we consolidated and completed these previous investigations in using large database of in situ measurements (soil composition, soil moisture and observations concerning the presence or the absence of crust) and TerraSAR-X images at different radar incidence angle.

The main objective of this study is to analyze the potential of the TerraSAR-X radar sensor to characterize soil-surface parameters at the plot and within-plot scales. The effects of soil moisture, roughness, soil composition and slaking crust on the TerraSAR-X backscattering coefficient are analyzed only over agricultural plots.

## 2. MATERIAL AND METHODS

### 2.1. STUDY SITE

The study site is the Orgeval watershed (104 km²), which is located to the east of Paris (France; 48°51'N 3°07'E; Figure 1). The site has been managed since 1962 as an experimental basin for hydrological research by the Agricultural and Environmental Engineering Research Center

(CEMAGREF) research institute. The Orgeval watershed is mostly composed of agricultural plots intended for growing wheat and maize. It is flat and composed of loamy soils with average percentages of 17% clay, 78% silt, and 5% sand. This soil structure promotes crust development, which increases soil sealing and causes runoff [Boiffin et al., 1990; Eimberck, 1990].

## 2.2. SATELLITE DATA

### 2.2.1. SAR data:

Fourteen TerraSAR-X images (X-band) were acquired in 2009 and 2010 in Spotlight mode (pixel spacing ~1 m) with HH polarization and incidence angles of 25° and 50°. The incidence angles of each TerraSAR image are summarized in Table 1.

Radiometric calibration of the MGD (Multi Look Ground Range Detected) TerraSAR images was carried out using the following equation [Fritz, 2007]:

$$\sigma^{\circ} = (Ks \cdot DN^2 - NEBN) \cdot \sin(\theta) \qquad (1)$$

This equation transforms the digital number of each pixel DN (amplitude of the backscattered signal) into a backscattering coefficient ($\sigma^{o}$) corrected for sensor noise (NEBN) on a linear scale. This calibration takes into account the radar incidence angle ($\theta$) and the calibration constant (Ks) provided in the image data. The backscattering coefficients are then calculated in decibels by the following formula:

$$\sigma^{o}_{dB} = 10 \cdot \log_{10} (\sigma^{\circ}) \qquad (2)$$

This radiometric calibration makes it possible to perform multi-temporal analysis of the different images. All of the images were then co-registered using aerial orthophotos (50-cm spatial resolution) with a root mean square error of the control points of approximately one pixel (i.e., 1 m). This co-registration error was overcome by removing the boundary pixels (two pixels wide) from each training plot relative to the limits defined by the GPS control points.

#### 2.2.2. Optical data:

One optical IKONOS image was acquired on March 14, 2009 in multispectral mode (pixel spacing ~ 4 m). The IKONOS image was calibrated for TOA (top of atmosphere) reflectance and co-registered using aerial orthophotos with a root mean square error of the control points of approximately one pixel (i.e., 4 m).

### 2.3. EXPERIMENTAL MEASUREMENTS

Simultaneously to the TerraSAR-X acquisitions, ground measurements were performed in thirteen bare training plots in 2009 and 2010 (± three hours around the satellite overpass time) (Figure 2). All training plots were flat (slope < 1%). Four soil-surface parameters were observed or measured: moisture content (at the 0-5-cm depth), surface roughness, soil composition, and slaking crust. Meteorological data (precipitation and temperature) were also obtained from five meteorological stations installed in the basin. Each station is less than 5 km from the center of each plot. Figure 3 shows the mean values of meteorological data recorded in 2009 (a) and 2010 (b) at the five stations.

#### 2.3.1. Soil roughness (*Hrms*):

Measurements of soil roughness were carried out in all of the training plots using 1-m-long needle profilometers with 2-cm sampling intervals. Ten roughness profiles along and across the direction of tillage (five parallel and five perpendicular) were established in each training plot. Two parameters can be calculated from these measurements: the average root mean square surface height (*Hrms*) and the correlation length (*l*) [Ulaby et al., 1986]. The *Hrms* values of the plots obtained during the two field surveys (March to May 2009 and March 2010) varied between 0.4 and 3.9 cm. The lower values (0.4 to 1.5 cm) corresponded to sown plots, whereas the higher values (above 1.5 cm) corresponded to fallow and recently ploughed plots. The correlation length (*L*) varies from 2.3 cm in sown fields to 9.3 cm in ploughed fields. As shown in Figure 4, the relationship between the *Hrms* and the correlation length can be modeled by a linear regression [Davidson et al. 2003, Baghdadi et al. 2008a]. Nevertheless, inverting the two parameters *Hrms* and *L* separately in the inversion of radar measurements seems to be a difficult task because our TerraSAR images contain a single band per pixel (one polarization and one incidence angle).

The error on the roughness computation is influenced mainly by the roughness profiles length, the number of profiles, and the horizontal resolution (sampling interval) of profiles.

According to Oh and Kay (1998), the roughness profiles length should be at least 40*L* and 200*L* (where *L* is the correlation length) in order to obtain the *Hrms* and the correlation length with a precision of 10%. Lievens et al. (2009) and Callens et al. (2006) have demonstrated that shorter profiles result in lower *Hrms* and correlation length. A significant underestimation of roughness parameters is observed for short profiles and large correlation length. The number of averaged profiles that is required to obtain a standard deviation on *Hrms* and *L* less than 10% is dependent of profile length. Lievens et al. (2009) demonstrated that less than 10 averaged profiles are required for 1 m profile to obtain a standard deviation of *Hrms* lower than 10%, whereas the same accuracy (better than 10%) for correlation length only becomes feasible for at least 15 averaged profiles. The precision on the correlation length measurements should be about 15 to 20% for the range of correlation length measured within our bare agricultural fields, with 1m profile and 10 average profiles (higher standard deviation for large correlation length). The precision associated with the measurements of *Hrms* and *L*, were also dependent on the horizontal spacing between height points ($\Delta$x). Oh and Kay (1998) suggested that the surface should be sampled at a spacing

Author-produced version of the article published in Remote Sensing Of Environment, 2011, 115(8), 1801-1810.
The original publication is available at http://www.sciencedirect.com/
doi : 10.1016/j.rse.2011.02.021

no longer than 0.2*L* and no more than 0.5*L* for the same precision of about 5% on the correlation length and the *Hrms* surface height, respectively. For our range of correlation length, the accuracy of roughness parameters with a spacing of 2 cm should be better than ± 10% for *Hrms* and between ± 10% and ± 20% for large and small correlation lengths, respectively. According to Lievens et al. (2009), an increase in horizontal spacing causes a decrease in *Hrms* and an increase in correlation length, which are more pronounced for surfaces with small correlation length. Moreover, the standard deviation of roughness parameters with a spacing of 1.5 cm is better than ±5% for *Hrms* and better than ±15% for correlation length.

Also, only the relationship between the *Hrms* surface height and the radar signal was used in this study; ten 1-m-long profiles are not sufficient to estimate *L* parameter with accuracy lower than 15% [Oh & Kay, 1998].

Finally, most of our training plots don't have marked row directions because they correspond to old winter ploughed without row direction (isotropic surface).

#### 2.3.2. Soil moisture (*mv*):

In most studies of microwave measurements carried out over bare soils, experimental relationship between soil moisture and backscattering coefficient are provided by mean volumetric water contents measured to a soil depth, generally 0-5 cm. At X-band, no experimental measurements were conducted in field condition and the low penetration of this radar wavelength is only based on theoretical study. So, the penetration depth of the X-band is not yet known.

In this study, between fifteen and twenty-eight gravimetric soil-moisture samples (depth: 0-5 cm) were collected per day for each training plot. The location of each gravimetric measurement was recorded using a GPS device.

Author-produced version of the article published in Remote Sensing Of Environment, 2011, 115(8), 1801-1810.
The original publication is available at http://www.sciencedirect.com/
doi : 10.1016/j.rse.2011.02.021

All gravimetric measurements were converted into volumetric moisture (*mv*) based on bulk density. Five bulk-density measurements were made for each training plot using 9-cm-long cylindrical samples with volumes of 500 $cm^{-3}$. Bulk-density values varied between 0.9 and 1.4 $g.cm^{-3}$. The soil moisture of each plot (or part of a plot) was assumed to be equal to the mean value estimated from the samples collected in that plot (or part of a plot). The two field surveys in 2009 and 2010 covered a large range of soil moisture, between 12.6% and 39.8% (see Table 1). The standard deviation of soil moisture measurements varied between 0.6% and 2.75%per each training plot (or part of a plot).

### **2.3.3. Soil composition**:

Soil composition was analyzed only in the training plots studied in 2009. For each training plot, ten soil samples were analyzed for their percentages of clay, sand and silt. The analysis showed that the surface soils within the training plots could be classified into two categories of loam:

- soil I: clay = 24% ± 1.9%; silt = 71% ± 1.7%; sand = 5% ± 1.5%.
- soil II: clay = 16% ± 0.9%; silt = 78% ± 2%; sand = 6% ± 1.3%.

The major differences between these two soils corresponded to small variations in clay and silt content (clay = 8%, silt = 7%). The largest difference in clay content between soil I and soil II was found in plot D (~10%), and the smallest value was found in plot G (~3%). The differences in sand content were very small (mean ~1%).

### **2.3.4. Slaking crust:**

The structure of bare soils can be modified by the energy of impact of raindrops, and a slaking crust can be formed on the soil surface. A slaking crust decreases the infiltrability of the soil,

Author-produced version of the article published in Remote Sensing Of Environment, 2011, 115(8), 1801-1810.
The original publication is available at http://www.sciencedirect.com/
doi : 10.1016/j.rse.2011.02.021

favoring runoff. This phenomenon is commonly observed on loamy soils and is dependent on soil composition (clay and silt content, organic matter and carbonate content).

The presence or absence of slaking crust on the soil surface was noted during the 2009 field survey. Slaking crust blocks the porosity of the soil surface, creating a layer of compacted soil that is often visible to the naked eye. The stagnation of water and the presence of a thin, continuous and consistent surface layer (crust) indicate the spatial extent of the slaking crust.

In March 2009, we observed slaking crust with a thickness of approximately 1 cm on soil II (16% ± 0.9% clay, 78% ± 2% silt and 6% ± 1.3% sand). In April and May 2009, no slaking crusts were observed within the training plots due to tillage operations that had removed the soil crusts and increased the porosity of the topsoil.

## 3. RESULTS

### 3.1. TERRASAR-X SIGNAL AND SOIL-SURFACE ROUGHNESS

For bare soils, surface roughness plays an important role in the amount of energy returned to the radar instrument. The sensitivity of the TerraSAR-X signal (σ°) in HH polarization to surface roughness (*Hrms*) at the plot scale was analyzed for both incidence angles (25° and 50°). The database was classified into three soil-moisture groups: $10\% < m_v < 15\%$ (low), $15\% < m_v < 25\%$ (medium) and $25\% < m_v < 40\%$ (high). For each incidence angle and soil-moisture group, the relationship between σ° and *Hrms* was analyzed.

For high soil moisture, σ° could be modeled by a logarithmic function according to *Hrms* for either incidence angle (Figures 4a and 4b), and σ° was more sensitive to surface roughness at a high incidence angle (50°) than at a low incidence angle (25°). The mean difference between the σ° values of the smoothest (*Hrms* = 0.7 cm) and roughest areas (*Hrms* = 3 cm) reached a maximum of 1.9 dB at 25° (Figure 5a) and approximately 3.5 dB at 50° (Figure 5b). Similar dynamics of the

Author-produced version of the article published in Remote Sensing Of Environment, 2011, 115(8), 1801-1810.
The original publication is available at http://www.sciencedirect.com/
doi : 10.1016/j.rse.2011.02.021

TerraSAR-X signal and surface roughness have been observed by Baghdadi et *al.* (2008a). Moreover, at an incidence angle of 25°, the backscattering coefficient quickly reaches its maximum level for an *Hrms* of approximately 0.8 cm (Figure 5a). Beyond this threshold, the backscattering coefficient becomes constant regardless of the roughness. Roughness values of less than 0.8 cm are rare in agricultural areas. Therefore, for agricultural applications, soil-roughness mapping is not feasible using X-band SAR data at a low incidence angle.

For medium soil moisture, the backscattering coefficient was almost constant for *Hrms* surface heights between 1.1 and 2.7 cm at either incidence angle (Figures 4a and 4b).

The lack of roughness data for low soil-moisture conditions made it possible to perform only partial observations for the 50° incidence angle. As observed for medium soil moisture, σ° values for low soil moisture seem to be independent of surface roughness for *Hrms* surface heights between 1.1 and 2.7 cm (Figure 5b).

The backscattering coefficients of soils with the same roughness but different soil-moisture levels (medium and high) were also compared. At a 25° incidence angle and for *Hrms* values between 1.1 and 2.7 cm, the backscattering coefficient of a soil with medium moisture content was approximately 4.0 dB lower than that of the same soil with high moisture content (Figure 5a). This difference of 4.0 dB was larger than that observed between smooth (*Hrms* ~ 0.4 cm) and rough (*Hrms* ~ 3 cm) soils (1.9 dB). At a 50° incidence angle and for *Hrms* surface heights between 0.8 and 2.7 cm, the backscattering coefficient of a soil with medium moisture content was approximately 1.5-5 dB lower than that of the same soil with high moisture content (Figure 5b). The difference in the backscattering coefficient between soils with different levels of moisture was smaller than the dynamics of the backscattering coefficient with changes in roughness at high soil moisture (3 dB for *Hrms* values between 0.8 and 2.7 cm, Figure 5b) for the smoothest areas and larger for the roughest areas. The lack of roughness data with low moisture content made it possible to perform only partial observations. At a 50° incidence angle and for *Hrms* values

Author-produced version of the article published in Remote Sensing Of Environment, 2011, 115(8), 1801-1810.
The original publication is available at http://www.sciencedirect.com/
doi : 10.1016/j.rse.2011.02.021

between 1.2 and 2.9 cm, the backscattering coefficient for low soil moisture was lower by approximately 4-6 dB than that of soils with high soil moisture (Figure 5b). This difference was larger than the difference in backscattering coefficient between soils with different levels of roughness at high soil moisture (2.1 dB for *Hrms* between 1.2 cm and 2.9 cm, Figure 5b).

In conclusion for agricultural bare plots, the effects of soil roughness on the TerraSAR-X signal are small and function of the moisture content. Consequently, the backscattering coefficient σ° (dB) in the X-band cannot be expressed as the sum of one function dependent on soil moisture and another dependent on *Hrms* surface height, as is commonly assumed for the L- and C-bands [Baghdadi et al., 2006; Zribi & Deschambre, 2002].

### 3.2. TERRASAR-X SIGNAL AND SOIL MOISTURE CONTENT

The high spatial resolution of the TerraSAR data (1 m) made it possible to analyze the radar signal according to soil moisture at the plot and within-plot scales. The mean backscattering coefficient was estimated for each training plot according to the scale of interest and plotted as a function of in situ soil-moisture measurements regardless of roughness. Figure 6 illustrates the dynamics of the radar backscattering coefficient versus soil moisture for HH polarization at low (25°) and high (50°) incidence angles. Overall, the scattering behavior of the soil increased with soil moisture. The wide range of soil-moisture measurements (13-40%) made it possible to establish linear relationships between the radar signal and the soil moisture for each incidence angle. The sensitivity of the radar signal to soil moisture was 0.411 dB/% for the TerraSAR-X data at 25° (Figure 6a). Paris Anguela et al. (2010) have observed a sensitivity of the same order using a single TerraSAR-X image and simulated data from the IEM model (X-HH-26°: 0.35 dB/%). For the high incidence angle (50°), the sensitivity of the TerraSAR-X signal to soil moisture decreased to 0.323 dB/% (Figure 6b). This analysis demonstrates that the SAR signal in the X-band is slightly more sensitive to soil moisture at a low incidence angle (25°), but soil-moisture mapping

Author-produced version of the article published in Remote Sensing Of Environment, 2011, 115(8), 1801-1810.
The original publication is available at http://www.sciencedirect.com/
doi : 10.1016/j.rse.2011.02.021

can be carried out with either low or high incidence angles (because both showed high sensitivities). This decreasing radar sensitivity with increasing incidence angle is consistent with other studies performed using C-band SAR data. Indeed, several studies using C-band data (ERS, RADARSAT, ASAR) have shown higher sensitivities between the radar signal and soil moisture for low incidence angles (0.2-0.3 dB/%) than for high incidence angles (0.1 dB/%) [Baghdadi et al., 2008a; Le Hégarat et al., 2002; Quesney et al., 2000; Srivastava et al., 2003]. Finally, the sensitivity of the radar signal to soil moisture appears to be higher in the X-band than in the C-band, regardless of the incidence angle. Theoretical surface backscattering models show approximately the same sensitivity between radar signal and soil moisture for these two radar wavelengths (Fung, 1994). The increasing in the sensitivity of radar signal to soil moisture at X-band could be due particularly to volume scattering effect. First, radar signal increases with soil moisture for C- and X-bands. In the other hand, the volume scattering term is certainly higher at C-band than at X-band for low and medium moistures due to more important penetration of waves. This means that at C-band, the dynamic of radar signal with soil moisture variation could be lower at C-band because of this scattering term added for low and medium soil moistures. This decrease in radar dynamic induces a decreasing of sensitivity at C-band.

### 3.3. TERRASAR-X SIGNAL AND SOIL COMPOSITION

The sensitivity of the TerraSAR-X signal to soil composition was studied using images acquired in 2009 because the soil-composition analysis focused on the training plots measured in 2009. Heterogeneities within plots were observed in the TerraSAR-X images only on March 17 and 18, 2009 (Figures 2 and 7). These variations within the training plots were also observed in the IKONOS image (Figure 7j).

To investigate these differences, soil samples were taken in each training plot to determine the particle-size distribution within plots. According to the soil-composition analysis, the zones with

Author-produced version of the article published in Remote Sensing Of Environment, 2011, 115(8), 1801-1810.
The original publication is available at http://www.sciencedirect.com/
doi : 10.1016/j.rse.2011.02.021

low radar-signal values (darker zones) were more clayey (soil I: 24% clay, 71% silt and 5% sand) than the zones with high radar-signal values (brightest zones; soil II: 16% clay, 78% silt and 6% sand). Also, the variations in the TerraSAR-X signal within plots were spatially correlated with the variations in soil composition on the two acquisition dates (March 17 and 18).

The mean differences in σ° between soil-II zones and soil-I zones had the same order of magnitude for the HH-25° (March 17: 2.6 dB) and HH-50° (March 18: 2.3 dB) configurations. Indeed, these two acquisitions occurred within an interval of less of 24 hours (ensuring the same surface conditions). Thus, according to these observations, the TerraSAR-X data allow to map limits of our two soils within the plots regardless of the incidence angle.

Simulations using the IEM radar-backscattering model [Fung, 1994] were also carried out for the two soil compositions (I and II). The surface-roughness (*Hrms*, *l*) and soil moisture *(mv)* values measured during the field survey were used to run the simulations. In the IEM model, the Hallikainen equations [Hallikainen et al., 1985] are used to calculate the dielectric constant according to the percentages of sand and clay. Our results showed that the X-band data did not discriminate the two soil categories (the variations between these soil categories were less than 1 dB in the X-band). These results were expected because the difference in soil composition between soil categories II and I was small. Indeed, the two soil compositions measured within the plots had a maximum mean difference in clay content of approximately 10% (training plot D). Several studies in the C- and L-bands have shown that the radar signal is directly dependent on the amount of sand and clay, but only for soil compositions that are very different (differences in clay content of more than 30%) [Dobson & Ulaby, 1981; Schmugge et al., 1976; Ulaby et al., 1978].

Similarly, the mean differences in sand content between the two soil categories did not exceed 1%. Prakash et al. (2009) has shown that the specular-scattering coefficient of X-band bistatic scatterometer data at HH polarization is strongly dependent on the percentage of sand in the soil when the surface is smooth. The change in the specular-scattering response with variations in soil

Author-produced version of the article published in Remote Sensing Of Environment, 2011, 115(8), 1801-1810.
The original publication is available at http://www.sciencedirect.com/
doi : 10.1016/j.rse.2011.02.021

composition is difficult to observe when the soil is rough (*Hrms* > 1.4 cm). On March 2009, the smoothest training plots had a roughness of approximately 1.9 cm. Therefore, changes in scattering with changes in soil composition within our rough plots were not clear in the TerraSAR data.

Thus, the TerraSAR-X signal was not directly sensitive to the soil composition in our training plots. Nevertheless, the spatial variation in the TerraSAR signal at the within-plot scale was correlated with the spatial distribution of soil composition in some TerraSAR-X acquisitions. Therefore, soil composition should affect other soil parameters that directly influence the TerraSAR-X signal.

### 3.4. TERRASAR-X SIGNAL AND SOIL CRUST

During the field survey in March 2009, slaking crust was observed on soil II and not on soil I. We studied the effect of the soil-II crust on the radar signal for seven training plots of 2009. Because soil crusts modify the water-retention properties and infiltration rates of the soil [Augeard, 2006; Musy & Soutter, 1991], the differences in soil moisture between soil II and soil I ($mv_{soil\ II}$ - $mv_{soil\ I}$) were compared to the differences in the TerraSAR signal ($\sigma°_{soil\ II}$ - $\sigma°_{soil\ I}$). The acquisitions on March 17 and 18, 2009 differed from the other 2009 acquisitions by their greater variation in signal and soil moisture within the training plots. The mean difference in signal calculated from the March 17 and March 18 images between the soil-II and soil-I zones was approximately +2.5 dB (Table 3) for a mean difference in moisture content of approximately +4.5% (2.9-7.2%, depending on the training plot) (Table 2). The difference in soil moisture between soils I and II can be explained by the difference in the soil-surface structure (i.e., the presence or absence of slaking crust). During the winter dry period (March 11 to March 22, Figure 3), soil I dries faster than soil II. In soil II, evaporation is limited by the crust, and the moisture content is retained longer than in soil I. Thus, the moisture-content values of soil I were lower than those of soil II. Because the

Author-produced version of the article published in Remote Sensing Of Environment, 2011, 115(8), 1801-1810.
The original publication is available at http://www.sciencedirect.com/
doi : 10.1016/j.rse.2011.02.021

TerraSAR signal is highly sensitive to soil moisture (section 3.2), the variations in moisture content between the two soils generated differences in the backscattered signal.

On March 25 and 26, the mean difference in signal between soil-II and soil-I zones was less than 1 dB (Table 3) for an average difference in moisture content of less than 1% (Table 2). Thus, no variation in either soil moisture or TerraSAR-X signal was observed within the plots on these dates. After rainy events (2.7 mm on March 23 and 4.7 mm only three hours before the March 25 acquisition; Figure 3), the moisture content of soil I increased strongly (by approximately +4.5%) because soil I absorbed both precipitation and streaming water coming from soil II. The moisture content of soil II increased slightly (by approximately 1%) because the soil crust prevented water infiltration and favored hydric inertia. On March 17 and 18, soil II had greater moisture content than soil I. Because the moisture content of soil I increased and the moisture content of soil II stayed constant, the difference in moisture content between the two soils disappeared. For the other acquisition dates between April 8 and May 11, 2009, tillage had destroyed the soil crust and increased the porosity of soil II. Without crust, the compositions of the two soils were too similar to generate a difference in moisture content between soil I and soil II (< 1%), and no differences in signal were observed between the two soils.

Thus, variations in the TerraSAR-X signal within plots were correlated with differences in the soil-surface structure between the two soils. The slaking crust on soil II generated differences in moisture content between soil I and soil II under certain conditions. For a single training plot located within the same study area, Paris Anguela et al. (2010) have shown that a soil with a smaller percentage of clay (soil B: 17% clay, 79% silt and 4% sand) had a TerraSAR signal (HH-25°) 3 dB stronger than that of a more clayey soil (soil A: 32% clay, 64.5% silt and 3.5% sand). The driest upper millimeters of soil B and the low X-band penetration at high moisture content [Nolan & Fatland, 2003] were used to explain the difference in signal between soil B and soil A.

Author-produced version of the article published in Remote Sensing Of Environment, 2011, 115(8), 1801-1810.
The original publication is available at http://www.sciencedirect.com/
doi : 10.1016/j.rse.2011.02.021

## 4. CONCLUSIONS

This study analyzes the potential of high-spatial-resolution data from the TerraSAR-X sensor to monitor the soil-surface characteristics of bare agricultural soils (roughness, moisture, composition and structure) at plot and within-plot scales. The backscattering coefficients obtained from multi-temporal SAR acquisitions at HH polarization and two incidence angles (25° and 50°) were compared to ground observations and measurements. Our results are promising for retrieving soil moisture information from TerraSAR-X data and for monitoring the dynamics of slaking crust hydric states within plots. The results are summarized below.

- For high soil moisture (25 < $m_v$ < 40%), the sensitivity of the TerraSAR-X backscattering coefficient to soil roughness is slightly higher at a 50° incidence angle (3.5 dB) than at a 25° incidence angle (1.9 dB). Moreover, for either incidence angle, the variation in the radar signal with surface roughness is smaller for soils with moisture contents between 15% and 25% than for soils with moisture contents over 25%. The sensitivity of the TerraSAR signal at 25° to soil roughness for areas with high moisture content (25% < mv < 40%) is lower than the difference in signal between two areas with different moisture contents (15% < mv < 25% and 25% < mv < 40%). At 50°, the change in σ° with surface roughness for high soil moisture is larger than the variation in the signal between two smooth soils (*Hrms* ~ 0.8 cm) with different soil moisture levels (15% < mv <25% and 25% < mv < 40%) and is slightly smaller in the case of rough areas (*Hrms* ~ 2.7 cm). Therefore, in the X-band, a high incidence angle (50°) is the optimal configuration for soil-roughness monitoring in agricultural areas (bare soils).
- The sensitivity of the TerraSAR-X signal to soil moisture is greater at a low incidence angle than at a high incidence angle (25°: 0.411 dB/%; 50°: 0.323 dB/%). Thus, an increase in moisture content of approximately 5% generates an increase in the backscattered signal of approximately 2.0 dB at a 25° incidence angle and 1.6 dB at a 50° incidence angle.

- The X-band SAR signal is not sensitive to slight differences in soil composition in bare agricultural fields (the maximum differences in our plots were 10% in clay and 1% in sand). No direct influence of soil composition on the radar signal was observed. Nevertheless, two TerraSAR-X acquisitions have shown signal variations within reference plots in the Orgeval study site that are spatially correlated with differences in soil composition at both high (50°) and low (25°) incidence angles (March 17 and 18, 2009). No TerraSAR-X signal variations were observed without crust or when there were no contrast of soil moisture between the soil crusted (II) and not crusted (I). So, when variations of composition engender variations of soil moisture (due to variations of soil structure and meteorological conditions), the spatial extent of soil composition can be observed within plots on TerraSAR-X signal.
- Variations in the TerraSAR-X signal within reference plots are correlated with the hydric evolution of soil crust. Soil with slaking crust (soil II) has a greater hydric inertia than soil without crust (soil I). Consequently, following rainfall or dry events, soil moisture in the upper centimeters may differ between the two soil structures, resulting in variations in the TerraSAR-X signal within the field. Thus, it is sometimes possible to track surface degradation due to the slaking process using the TerraSAR-X sensor.

Because of the low sensitivity to surface roughness and the high sensitivity to soil moisture, the use of TerraSAR-X data at HH polarization with a single incidence angle is a promising method for estimating soil parameters. Further studies are needed to analyze the complementary polarizations and incidence angles. Similarly, the synergy between the X-band (TerraSAR-X) and other SAR wavelengths (PALSAR/ALOS, RADARSAT-2, ASAR/ENVISAT) should be examined.

**Acknowledgments**

Author-produced version of the article published in Remote Sensing Of Environment, 2011, 115(8), 1801-1810.
The original publication is available at http://www.sciencedirect.com/
doi : 10.1016/j.rse.2011.02.021

The authors wish to thank DLR (the German Space Agency) for kindly providing the TerraSAR-X images (proposal HYD0007 and HYD0542). We extend our thanks to Noveltis and CNES (the French Space Study Center), which financed this study. We also thank S. Follain for helping to interpret the soil results, Elie Saba for helping to compute IEM simulation and P. Ansart, G. Tallec and Y. Hachouch for helping to collect field data.

## References

**Aly, Z., Bonn, F. J., Magagi, R. (2007)**. Analysis of the backscattering coefficient of salt-affected soils using modeling and radarsat-1 SAR data. *IEEE Transactions on Geoscience and Remote Sensing, vol. 45, n° 2: 332 – 341*

**Augeard, B. (2006).** Mécanismes de genèse du ruissellement sur sol agricole drainé sensible à la battance. Etudes expérimentales et modélisation. *Doctorat Sciences de l'eau, Unité de Recherche Hydrosystèmes et Bioprocédés, ENGREF 06ENGR0010, 236 p.*

**Auzet, A.V., Kirkby, M.J., Van Dijk, P. (2005).** Surface characterisation for soil erosion forecasting. *Catena, vol. 62, n° 2–3: 77–78.*

**Baghdadi, N., Gaultier, S., King, C. (2002).** Retrieving surface roughness and soil moisture from SAR data using neural network. *Canadian Journal of Remote Sensing vol. 28, n° 5: 701–711.*

**Baghdadi, N., Holah, N., Zribi, M., (2006).** Soil moisture estimation using multi-incidence and multi-polarization ASAR SAR data. *International Journal of Remote Sensing, vol. 27, n° 10: 1907–1920.*

**Baghdadi, N., Aubert, M., Cerdan, O., Franchistéguy, L., Viel, C., Martin, E., et al. (2007).** Operational mapping of soil moisture using synthetic aperture radar data: application to Touch basin (France). *Sensors Journal, vol. 7: 2458−2483.*

Author-produced version of the article published in Remote Sensing Of Environment, 2011, 115(8), 1801-1810.
The original publication is available at http://www.sciencedirect.com/
doi : 10.1016/j.rse.2011.02.021

**Baghdadi, N., Zribi, M., Loumagne, C., Ansart, P., & Paris Anguela, T. (2008a).** Analysis of TerraSAR-X data and their sensitivity to soil surface parameters over bare agricultural fields. *Remote sensing of Environnement, vol. 112, n° 12: 4370-4379.*

**Baghdadi, N., Cerdan, O., Zribi, M., Auzet, V., Darboux, F., El Hajj, M., et al. (2008b).** Operational performance of current synthetic aperture radar sensors in mapping soil surface characteristics*:* application to hydrological and erosion modelling. *Hydrological Processes, vol. 22, n° 1: 9−20.*

**Beaudoin, A., Gwy, Q.H.J., Le Toan, T. (1990).** SAR observation and modelling of the C-band backscatter variability due to multi-scale geometry and soil moisture. *IEEE Transactions on Geoscience & Remote Sensing, vol. 28:* 886-894.

**Boiffin, J., Papy F., & Eimberck, M. (1988).** Influence des systèmes de culture sur les risques d'érosion par ruissellement concentré : Analyse des conditions de déclenchement de l'érosion. *Agronomie, vol. 8: 663-673.*

**Callens, M., Verhoest, N., Davidson, M. (2006).** ParametrizationCondition for precise measurement of soil surface roughness. *IEEE Transactions on Geoscience and Remote Sensing, vol. 36, n° 2: 691 – 695.*

**Cerdan, O., Poesen, J., Govers, G., Saby, N., Le Bissonnais, Y., Gobin, A., Vacca, A., Quinton, J., Auerswald, K., Klik, A., Kwaad, F.J.P.M., Roxo, M.J. (2006).** Sheet and rill erosion rates in Europe. *In soil Erosion in Europe, Boardman J., Poesen J (eds), chap. 38. Wiley* : *Chichester, UK: 501–513.*

**Davidson, M., Mattia, F., Satalino, G., Verhoest, N., Le Toan, T., Borgeaud, M., Louis, J., Attema, E. (2003).** Joint statistical properties of RMS height and correlation length derived from multisite 1-m roughness measurements. *IEEE Transactions on Geosciences and Remote Sensing, vol. 41: 1651-1658.*

**Dobson, M.C., & Ulaby, F.T. (1981).** Microwave backscatter dependence on surface roughness, soil moisture and soil texture: Part III- soil tension. *IEEE Transactions on Geosciences and Remote Sensing, vol. 19: 51-61.*

**Dobson, M.C., & Ulaby, F.T. (1986).** Active microwave soil moisture research. *IEEE Transactions on Geoscience and Remote Sensing, vol. GE-24, n° 1: 23-36.*

**Eimberck, M. (1990).** Facteurs d'érodibilité des sols limoneux: réflexions à partir du Pays de Caux. Cah. (In French.). *ORSTOM, série Pédologique, vol. XXV, n° 1-2: 81–94.*

**Fung, A.K., & Chen, K.S. (1992).** Dependence of the surface backscattering coefficients on roughness, frequency and polarization states. *International Journal of Remote Sensing, vol. 13: 1663-1680.*

**Fung, A,K. (1994)**. Microwave Scattering and Emission Models and their Applications. *Artech House, Norwood, Massachussetts* : *573 p.*

**Fritz, T. (2007).** TerraSAR-X Level 1b Product Format Specification", *TX-GS-DD-3307, n° 1.3.*

**Govers, G., Takken, I., Helming, K. (2000).** Soil roughness and overland flow, *Agronomie, vol. 20: 131-146.*

**Hallikaïnen, M., Ulaby, F., Dobson, F., El Rayes, M., & Wu, L. (1985).** Microwave dielectric behavior of wet soil. Part I : Empirical models and experimental observations, *IEEE Transactions on Geoscience and Remote Sensing, vol. 23: 25-34.*

**Holah, N., Baghdadi, N., Zribi, M., Bruand, A., & King, C. (2005).** Potential of ASAR/ENVISAT for the characterization of soil surface parameters over bare agricultural fields. *Remote Sensing of Environnement, vol. 96, n° 1: 78-86.*

**King, D., & Le Bissonnais, Y. (1992)**. Rôle des sols et des pratiques culturelles dans l'infiltration et l'écoulement des eaux . Exemple du ruissellement et de l'érosion sur les plateaux limoneux du nord de l'Europe. *C. R. Acad. FR., vol. 78, n° 6: 91-105.*

Author-produced version of the article published in Remote Sensing Of Environment, 2011, 115(8), 1801-1810.
The original publication is available at http://www.sciencedirect.com/
doi : 10.1016/j.rse.2011.02.021

**Lasne, Y., Paillou, Ph., Ruffié, G., Serradilla, C., Demontoux, F. (2008).** Effect of salinity on the dielectric properties of geological materials: implication for soil moisture detection by means of remote sensing. *IEEE Transactions on Geoscience and Remote Sensing, vol. 46, n° 6: 1674-1688.*

**Le Bissonnais, Y., & Singer, M.J. (1992).** Crusting, Runoff and erosion Response to soil Water Content and Successive Rainfalls. *Soil Science Society American Journal, vol. 56: 1898-1903.*

**Le Hégarat Mascle, S., Zribi, M., Alem, F., Weisse, A., & Loumagne, C. (2002).** soil moisture estimation from ERS/SAR data : toward an operational methodology. *IEEE Transactions on Geoscience and Remote Sensing, vol. 40, n° 12: 2647-2658.*

**Lievens, H., Vernieuwe, H., Alvarez-Mozos, J., De Baets, B., Verhoest, N., (2009).** Error in radar-derived soil moisture due to roughness parameterization: an analysis based on synthetical surface profiles. *Sensors Journal, vol. 9: 1067−1093.*

**Loumagne, C., Michel, C., Normand, M. (1991).** Soil water conditions and forecasting rain water runoff. *Journal of Hydrology, vol. 123: 1-17.*

**Loumagne, C., Weisse, A., Normand, M., Riffard, M., Quesney, A.,Le Hegarat-Mascle, S., Alem, F. *(2001).*** Integration of remote sensing data into hydrological models for flood forecasting. *Remote Sensing and Hydrology 2000, IASH Red Book Pub., n°267, edited by Brubaker, Ritchie, Rango: 592-594.*

**Musy, A., et Soutter, M. (1991).** Physique du sol. *Presses Polytechniques et Universitaires Romandes, Lausanne, Suisse, 335p.*

**Nolan, M., & Fatland, D.R. (2003).**Penetration Depth as a DInSAR Observable and Proxy for soil Moisture. *IEEE Transactions on Geoscience and Remote Sensing, vol. 41, n° 3:532-537.*

**Oh, Y., & Kay, Y.(1998).** Condition for precise measurement of soil surface roughness. *IEEE Transactions on Geoscience and Remote Sensing, vol. 36, n° 2: 691 – 695.*

**Oh, Y. (2004).** Quantitative retrieval of soil moisture content and surface roughness from multipolarized radar observations of bare soil surfaces. *IEEE Transactions on Geoscience and Remote Sensing, vol. 42, n° 3: 596 – 601.*

**Oudin, L., Weisse, A., Loumagne, C., Le Hegarat-Mascle, S. (2003).** Assimilation of soil moisture into Hydrological models for flood forecasting a variational approach. *Canadian Journal of Remote sensing, vol. 29, n° 6: 679-686.*

**Paris Anguela, T., Zribi, M., Baghdadi, N., Loumagne, C. (2010).** Analysis of local variation of soil surface parameters with TerraSAR-X radar data over bare agricultural fields. *IEEE Transactions on Geoscience and Remote Sensing vol. 48, n° 2: 874–881.*

**Prakash, R., Singh, D., Pathak, N.P. (2009).** Microwave specular scattering response of soil texture at X-band. *Advances in Space Research, vol. 44, n° 7: 801–814.*

**Quesney, A., Le Hegarat-Mascle, S., Taconet, O., Vidal-Madjar, D., Wingneron, J.P., Loumagne, C., & Normand, M. (2000).** Estimation of watershed soil moisture index from ERS/SAR data. *Remote sensing of environment, vol. 72, n° 3: 290-303.*

**Schmugge, T., Wilheit, T., Webster, W., & Gloerson, P. (1976).** Remote sensing of soil moisture with microwave radiometers-II. *NASA Goddard Space Flight Center, Greenbelt, MD, 20771. NASA Technical Note TN-D-8321.*

**Shao, Y., Hu Q., Guo, H., Lu, Y., Dong, Q., Han, C. (2003).** Effect of dielectric properties of moist salinized soils on backscattering coefficients extracted from RADARSAT image. *IEEE Transactions on Geoscience and Remote Sensing, vol. 41: 1879 – 1888.*

**Shi, J., Wang, J., Hsu, A.Y., O'Neill, P.E., Engman, E.T. (1997).** Estimation of bare surface soil moisture and surface roughness parameter using L band SAR image data. *IEEE Transactions on Geoscience and Remote Sensing, vol. 35, n° 5: 1254–1266.*

Author-produced version of the article published in Remote Sensing Of Environment, 2011, 115(8), 1801-1810.
The original publication is available at http://www.sciencedirect.com/
doi : 10.1016/j.rse.2011.02.021

**Singh, D. (2005).** A simplistic incidence angle approach to retrieve the soil moisture and surface roughness at X-band. *IEEE Transactions on Geoscience and remote Sensing, vol. 43, n° 11: 2606-2611.*

**Srivastava, H.S., Patel, P., Manchanda, M.L., Adiga, S. (2003).** Use of multiincidence angle RADARSAT-1 SAR data to incorporate the effect of surface roughness in soil moisture estimation. *IEEE Transactions on Geoscience and Remote Sensing, vol. 41, n° 7: 1638–1640.*

**Srivastava, H.S., Patel, P., Navalgund, R.R., (2006).** Incorporating soil texture in soil moisture estimation from extended low-1 beam mode RADARSAT-1 SAR data. *International Journal of Remote Sensing, vol. 27, n°12-14: 2587– 2598.*

**Srivastava, H.S., Patel, P., Sharma, Y., Navalgund R.R. (2009).** Large area soil moisture estimation using multi-incidence-angle RADARSAT-1 SAR data. IEEE Transactions on Geoscience and Remote Sensing, vol. 47, n° 8: 2528–2535.

**Stolp, J., Janse, A.R.P. (1986).** X-band radar backscattering for detecting spatial distribution of soil slaking. *ITC Journal, vol. 1: 82-87.*

**Taylor, G. R., Mah, H.A., Kruse, F.A., Kierein-Young, K.S., Hewson, R.D., & Bennett, B.A. (1996).** Characterization of saline soils using airborne radar imagery. *Remote Sensing Environment, vol. 57: 127 - 142.*

**Ulaby, F.T., Batlivala, P.P., & Dobson, M.C. (1978).** Microwave backscatter dependence on surface roughness, soil moisture, and soil texture: Part I – Bare soil. *IEEE Transactions on Geoscience and Remote Sensing, vol. GE-16, n° 4: 286-295.*

**Ulaby, F.T., Moore, R.K., & Fung, A.K. (1986).** Microwave Remote Sensing, Active and Passive, From Theory to Applications, vol. 3, *Artech House, Inc., 685 Canton Street, Norwood, MA 02062, 1098 p.*

Author-produced version of the article published in Remote Sensing Of Environment, 2011, 115(8), 1801-1810.
The original publication is available at http://www.sciencedirect.com/
doi : 10.1016/j.rse.2011.02.021

**Valentin, C., Poesen, J., Li, Y. (2005).** Gully erosion: impacts, factors and control. *Catena vol. 63, n° 2–3: 132–153.*

**Valentin, C., & Bresson, L.M. (1992).** Morphology, genesis and classification of surface crusts in loamy and sandy soils. *Geoderma, vol. 55: 225-245.*

**Wu, Q., Wang, M. (2007).** A framework for risk assessment on soil erosion by water using an integrated and systematic approach. *Journal of hydrology, vol. 337: 11-21.*

**Zobeck, T.M., & Onstad, C.A. (1987).** Tillage and rainfall effects on random roughness: a review. *Soil & Tillage Research, vol. 9: 1-20.*

**Zribi, M., Dechambre, M. (2002).** A new empirical model to retrieve soil moisture and roughness from C-band radar data. *Remote Sensing of Environment, vol. 84: 42–52.*

**Zribi, M., Baghdadi, N., Holah, N., Fafin, O. (2005).** New methodology for soil surface moisture estimation and its application to ENVISAT-ASAR multi-incidence data inversion. *Remote Sensing of Environment, vol. 96: 485–496.*

Author-produced version of the article published in Remote Sensing Of Environment, 2011, 115(8), 1801-1810.
The original publication is available at http://www.sciencedirect.com/
doi : 10.1016/j.rse.2011.02.021

## Tables and Figures

*Table 1. Characteristics of TerraSAR images and in situ soil-moisture measurements.*

| SAR acquisition date dd/mm/yy | Incidence angle | In situ soil moisture (%) [Min; Max] |
|---|---|---|
| 17/03/09 | 25° | [24.7; 32.3] |
| 18/03/09 | 50° | [24.5; 29.8] |
| 25/03/09 | 50° | [24.1; 31.0] |
| 26/03/09 | 25° | [23.9; 32.7] |
| 08/04/09 | 25° | [16.8; 27.5] |
| 09/04/09 | 50° | [15.2; 26.3] |
| 17/04/09 | 25° | [14.1; 16.4] |
| 20/04/09 | 50° | [18.3; 23.9] |
| 11/05/09 | 25° | [25.8; 31.3] |
| 01/03/10 | 50° | [33.4; 39.8] |
| 02/03/10 | 25° | [32.7; 39.0] |
| 04/03/10 | 25° | [27.3; 34.3] |
| 12/03/10 | 50° | [12.6; 29.0] |
| 13/03/10 | 25° | [14.9; 26.3] |

*Table 2. Variations in soil moisture within the training plots (%). For each date and training plot, the difference in soil moisture between soil II and soil I is shown. Slaking crust was observed on soil II on March 17, 18, 25 and 26, 2009. N.A.: not available.*

| Training plot ID | TerraSAR-X acquisition date (dd/mm/yy) | | | | | | | | |
|---|---|---|---|---|---|---|---|---|---|
| | 17/03/09 HH-25° | 18/03/09 HH-50° | 25/03/09 HH-50° | 26/03/09 HH-25° | 08/04/09 HH-25° | 09/04/09 HH-50° | 17/04/09 HH-25° | 20/04/09 HH-50° | 11/05/09 HH-25° |
| A | N.A. | N.A. | N.A. | N.A. | N.A. | N.A. | 1.6 | 0.1 | N.A. |
| B | N.A. | 5.2 | N.A. | 2.7 | 0.5 | 1.4 | 0.9 | 0.2 | 0.2 |
| C | 4.7 | 3.7 | 0.5 | -1.6 | -1.4 | -0.3 | 1.0 | 0.6 | 1.1 |
| D | 5.1 | 7.2 | N.A. | 1.0 | N.A. | -1.4 | 0.1 | 0.4 | 0.4 |
| E | 3.1 | 2.9 | 0.2 | -1.0 | -0.4 | 0.1 | 0.1 | 0.7 | N.A. |
| F | N.A. | N.A. | N.A. | N.A. | N.A. | N.A. | N.A. | N.A. | N.A. |
| G | N.A. | N.A. | N.A. | N.A. | N.A. | N.A. | 0.7 | 0.9 | 0.1 |
| **Mean ($mv_{soil\ II}$ - $mv_{soil\ I}$) of training plots C, D, E** | **4.3** | **4.6** | **0.3** | **-0.5** | **-0.6** | **-0.5** | **0.4** | **0.6** | **0.7** |

Author-produced version of the article published in Remote Sensing Of Environment, 2011, 115(8), 1801-1810.
The original publication is available at http://www.sciencedirect.com/
doi : 10.1016/j.rse.2011.02.021

*Table 3. Variations in the TerraSAR-X signal within the training plots (dB). For each date and training plot, the difference between the radar signal of soil II and that of soil I is shown. Slaking crust was observed on soil II on March 17, 18, 25, and 26, 2009. N.A.: not available.*

| **Training plot ID** | **TerraSAR-X acquisition date (dd/mm/yy)** | | | | | | | | |
|---|---|---|---|---|---|---|---|---|---|
| | **17/03/09 HH-25°** | **18/03/09 HH-50°** | **25/03/09 HH-50°** | **26/03/09 HH-25°** | **08/04/09 HH-25°** | **09/04/09 HH-50°** | **17/04/09 HH-25°** | **20/04/09 HH-50°** | **11/05/09 HH-25°** |
| A | 1.6 | 1.5 | 0.5 | 0.8 | 0.3 | -0.1 | -0.2 | 0.1 | 1.4 |
| B | 2.7 | 2.1 | -2.3 | -0.7 | 0.6 | -0.4 | -0.5 | 0.5 | -0.6 |
| C | 2.4 | 2.3 | -0.1 | -0.1 | 0.4 | 0.3 | 0.1 | 0.7 | 0.3 |
| D | 2.6 | 2.3 | -1.1 | 0.1 | 0.7 | 0.8 | -0.5 | 0.6 | -0.2 |
| E | 2.8 | 2.3 | -0.4 | -0.2 | 0.8 | 1.3 | N.A. | 0.5 | 0.3 |
| F | 2.2 | 2.6 | 0.1 | -0.4 | 0.7 | 0.8 | -0.7 | N.A. | 1.2 |
| G | 1.1 | 1.1 | -0.5 | 0.1 | 0.7 | 0.8 | -0.1 | 0.9 | 0.1 |
| **Mean ($\sigma°_{soil\ II}$ - $\sigma°_{soil\ I}$) of training plots C, D, E** | **2.6** | **2.3** | **-0.5** | **-0.1** | **0.6** | **0.8** | **-0.2** | **0.6** | **0.1** |


*Figure 1. Location of the Orgeval watershed (France; central coordinates: 48°51'N, 3°07'E).*

Author-produced version of the article published in Remote Sensing Of Environment, 2011, 115(8), 1801-1810.
The original publication is available at http://www.sciencedirect.com/
doi : 10.1016/j.rse.2011.02.021

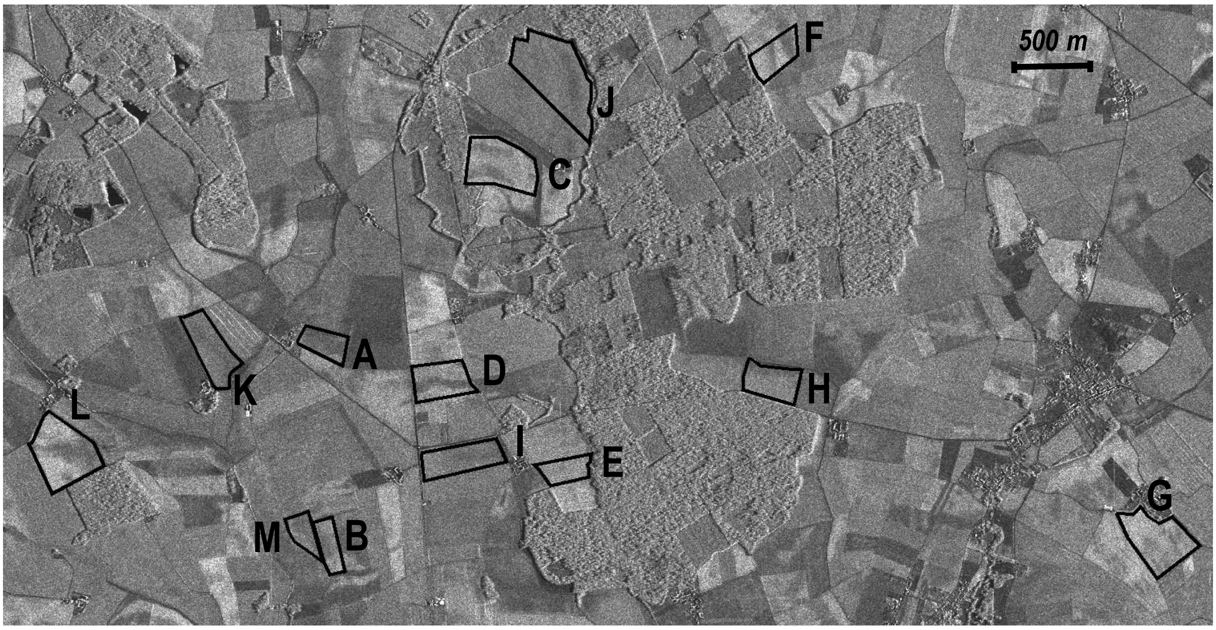


*Figure 2. A portion of a TerraSAR-X image (HH-25°, 17 March 2009) of the Orgeval site (central coordinates: 48°52'N, 3°06'E). Field surveys were performed in seven plots (A to G) in 2009 and six plots (H to M) in 2010. The reference plots are outlined in black.*

Author-produced version of the article published in Remote Sensing Of Environment, 2011, 115(8), 1801-1810.
The original publication is available at http://www.sciencedirect.com/
doi : 10.1016/j.rse.2011.02.021

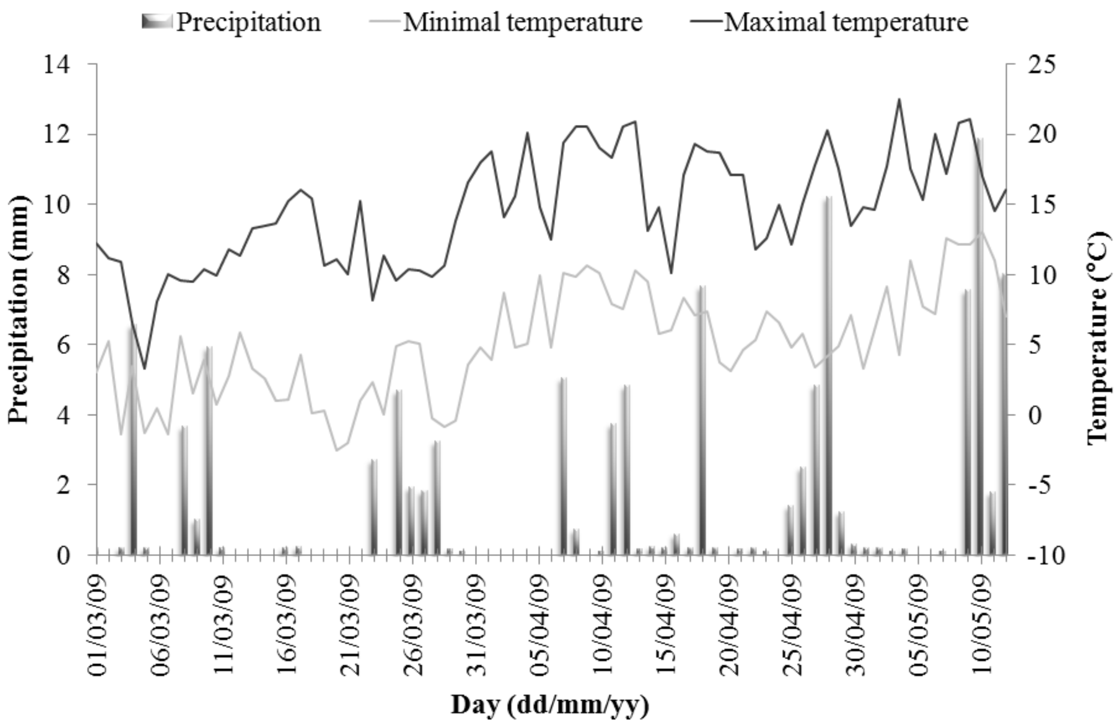


(a)

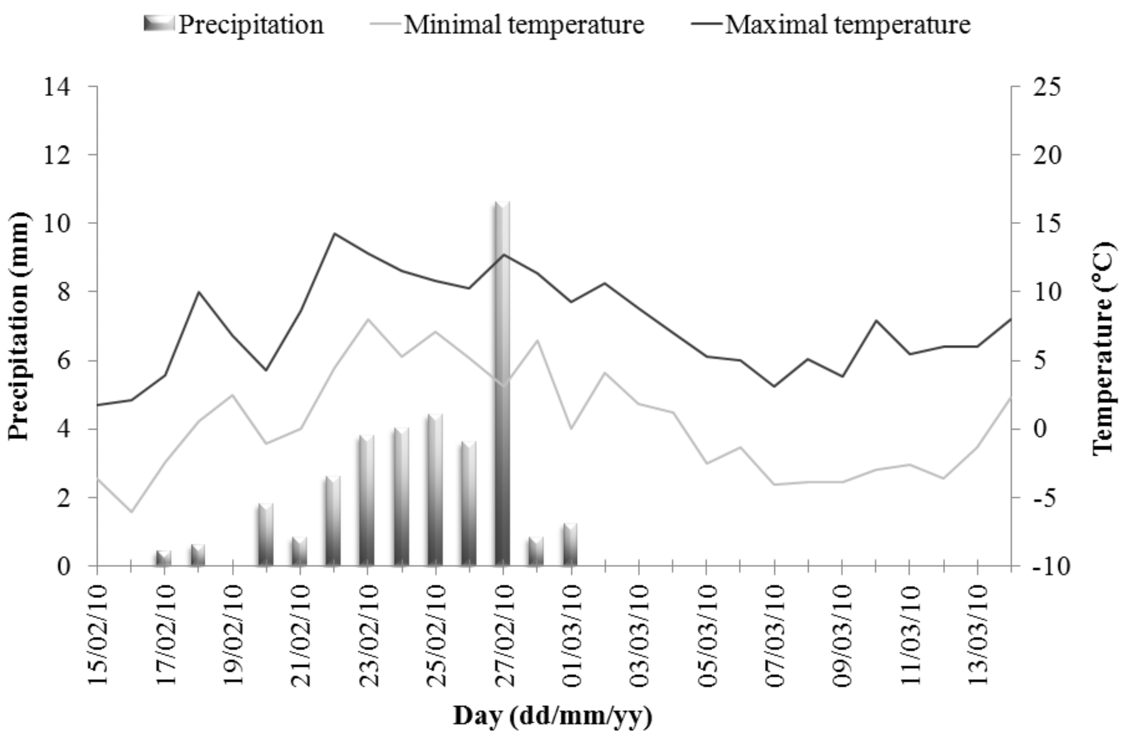


(b)

*Figure 3. Meteorological data averaged over the five stations installed in the basin: daily precipitation (mm) and minimum and maximum temperatures in 2009 (a) and 2010 (b).*

Author-produced version of the article published in Remote Sensing Of Environment, 2011, 115(8), 1801-1810.
The original publication is available at http://www.sciencedirect.com/
doi : 10.1016/j.rse.2011.02.021

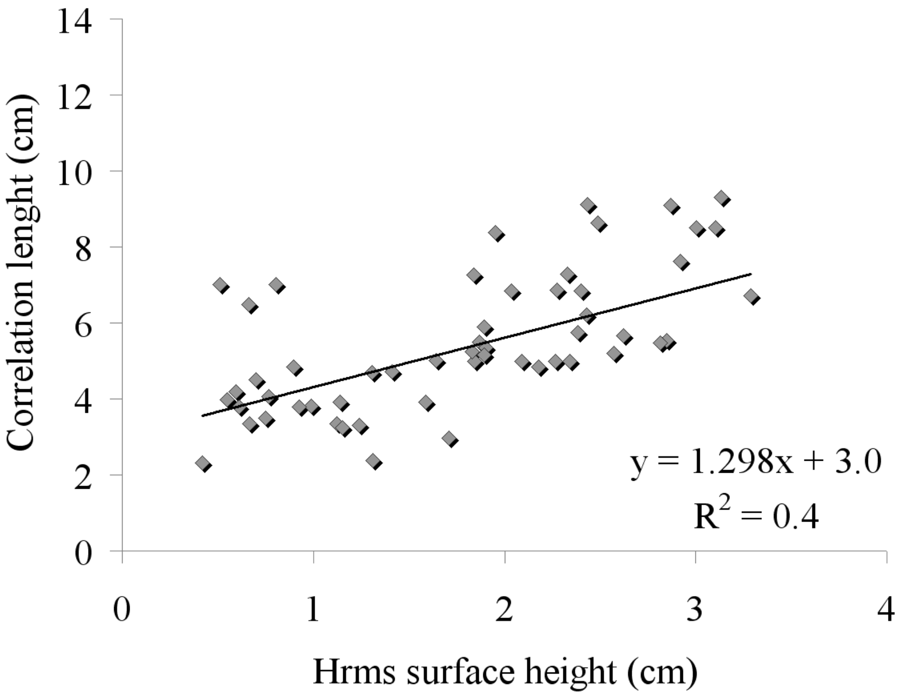


*Figure 4. Hrms surface height versus correlation length from measurements carried out in this campaign.*

Author-produced version of the article published in Remote Sensing Of Environment, 2011, 115(8), 1801-1810.
The original publication is available at http://www.sciencedirect.com/
doi : 10.1016/j.rse.2011.02.021

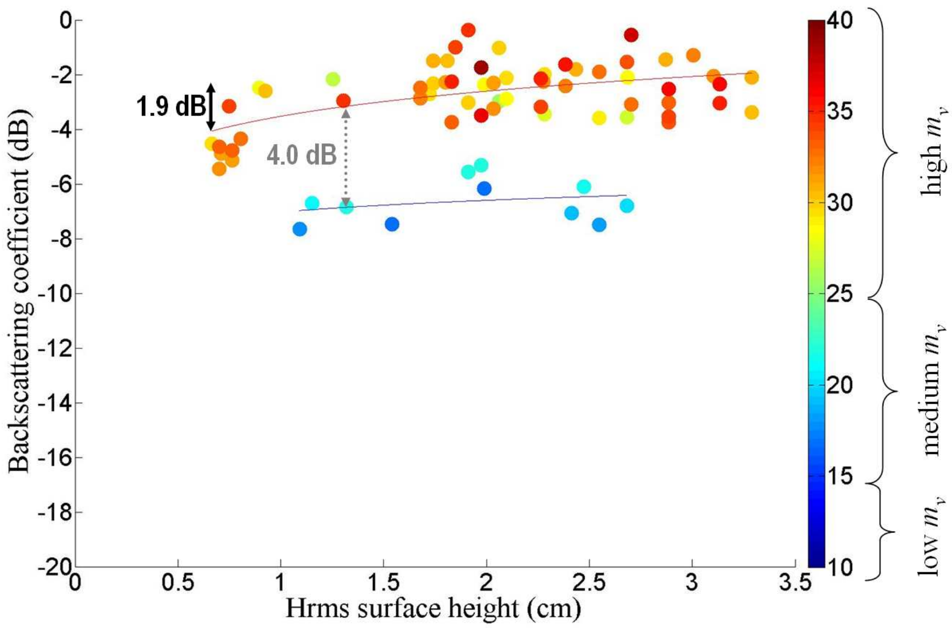


(a) medium *mv*: σ° = 0.62.ln(*Hrms*) - 7.0; $R^2$ = 0.1; RMSE = 0.7 cm
high *mv*: σ° = 1.32.ln(*Hrms*) - 3.5; $R^2$ = 0.3; RMSE = 0.9 cm

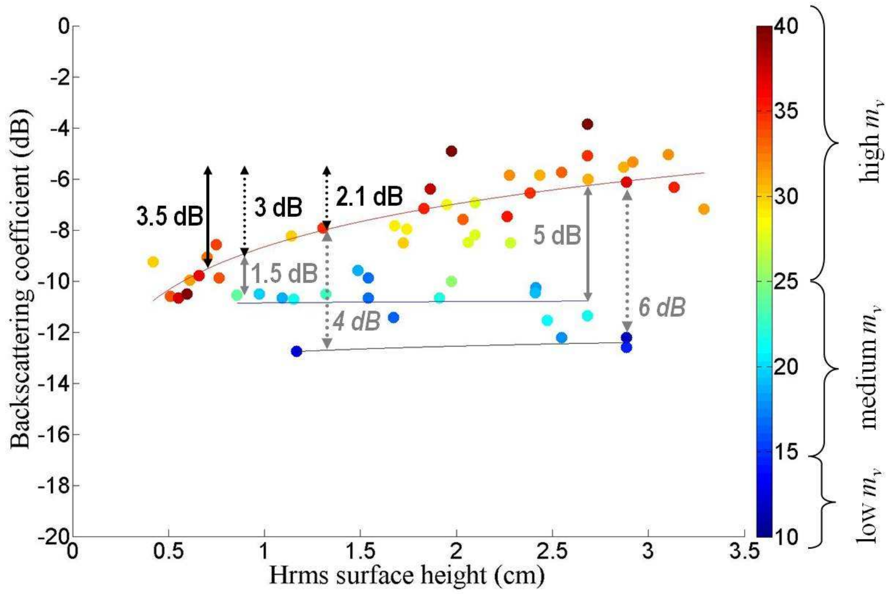


(b) low *mv*: σ° = 0.20.ln(*Hrms*) - 12.9; $R^2$ = 0.5; RMSE = 0.1 cm
medium *mv*: σ° = 0.01.ln(*Hrms*) - 10.3; $R^2$ = 0.1; RMSE = 0.6 cm
high *mv*: σ° = 2.43.ln(*Hrms*) - 08.7; $R^2$ = 0.7; RMSE =1.0 cm

*Figure 5. The sensitivity of the TerraSAR-X signal (at HH polarization) to soil roughness for incidence angles of 25° (a) and 50° (b). Each point corresponds to one training plot (mean values).*

Author-produced version of the article published in Remote Sensing Of Environment, 2011, 115(8), 1801-1810.
The original publication is available at http://www.sciencedirect.com/
doi : 10.1016/j.rse.2011.02.021

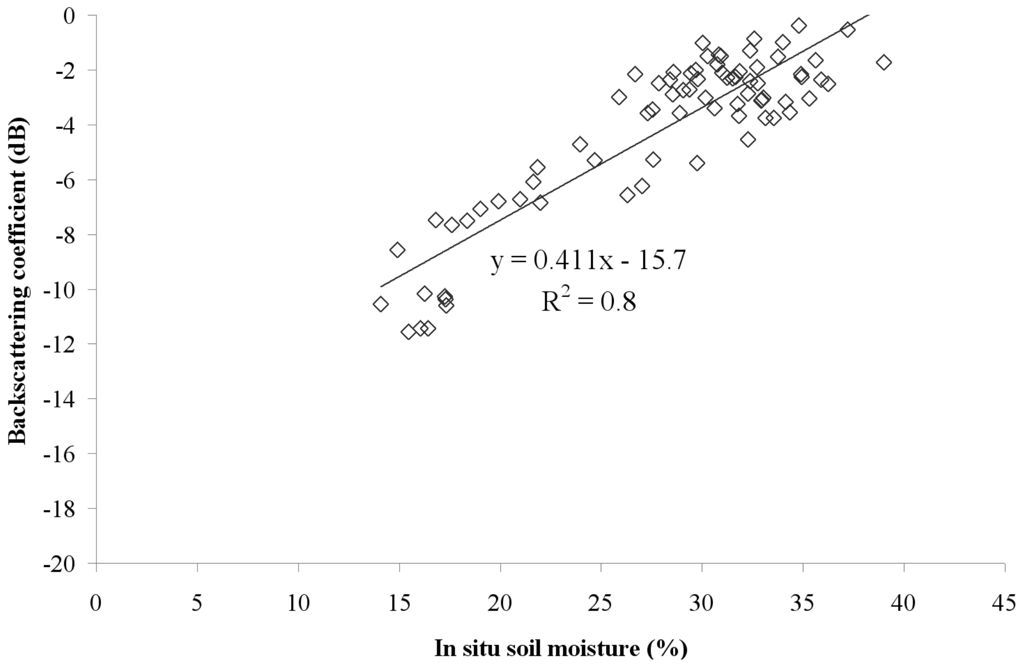


(a) RMSE =1.32%

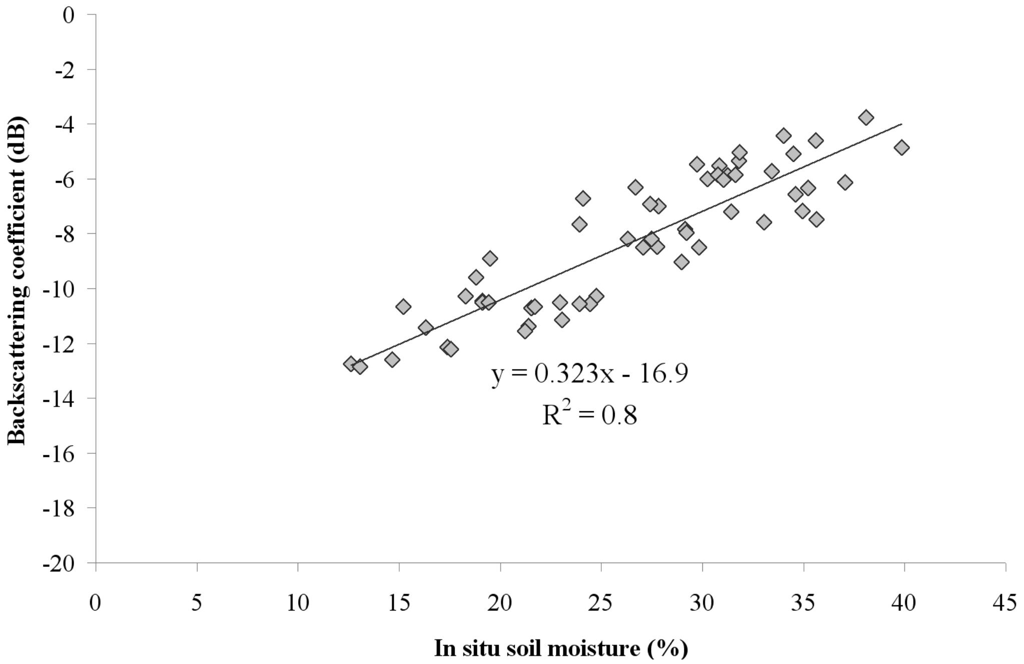


(b) RMSE =1.14%

*Figure 6. The sensitivity of the TerraSAR-X signal (at HH polarization) to soil moisture in the top 0–5-cm soil layer for incidence angles of 25° (a) and 50° (b). Each point corresponds to one training plot or portion of a plot.*

Author-produced version of the article published in Remote Sensing Of Environment, 2011, 115(8), 1801-1810.
The original publication is available at http://www.sciencedirect.com/
doi : 10.1016/j.rse.2011.02.021

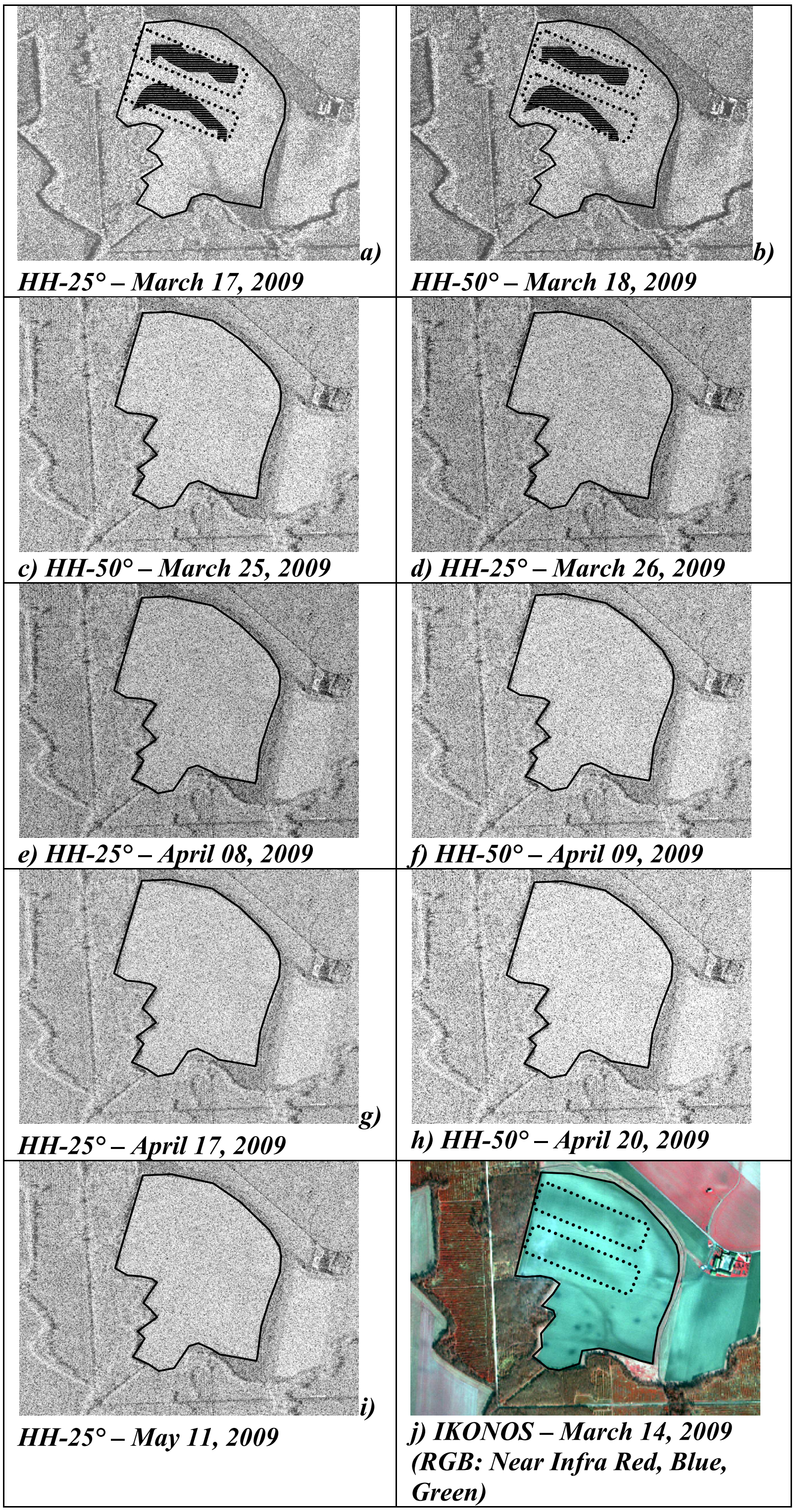


*Figure 7. Variations in signal strength within training plot C (outlined in black) for each TerraSAR-X acquisition (a-i). A subset of the IKONOS image acquired on March 14, 2009 is also shown (j). For the 17 and 18 March acquisitions, Soil I is outlined with a dotted black line (darker zone), and soil II corresponds to the brighter zones.*